An Anion Exchange Membrane of Layered Silicalite Nanosheets with Surface Quaternary Ammonium Cations

Yukta Sharma, Devraj Singh, Zishu Cao, Jan Gabski, Junhang Dong [*]

Department of Chemical and Environmental Engineering, University of Cincinnati, Cincinnati, OH 45221, USA.

*Corresponding author: dongj@ucmail.uc.edu

Appendix A. Supplementary Data

Fig. 1S (a) Simulated topological crystal structure of the MFI-type zeolite framework (Database of Zeolite Structures, Structure Commission of the International Zeolite Association 2017-2022), (b) structure and dimensions of the interconnected channels in the MFI-type zeolite, (c) depiction of the dC_5-templated pure-silica MFI-zeolite (silicalite) nanosheet (SN), and (d) depiction of an exposed QAC at a SN surface defect of incomplete unit cell.
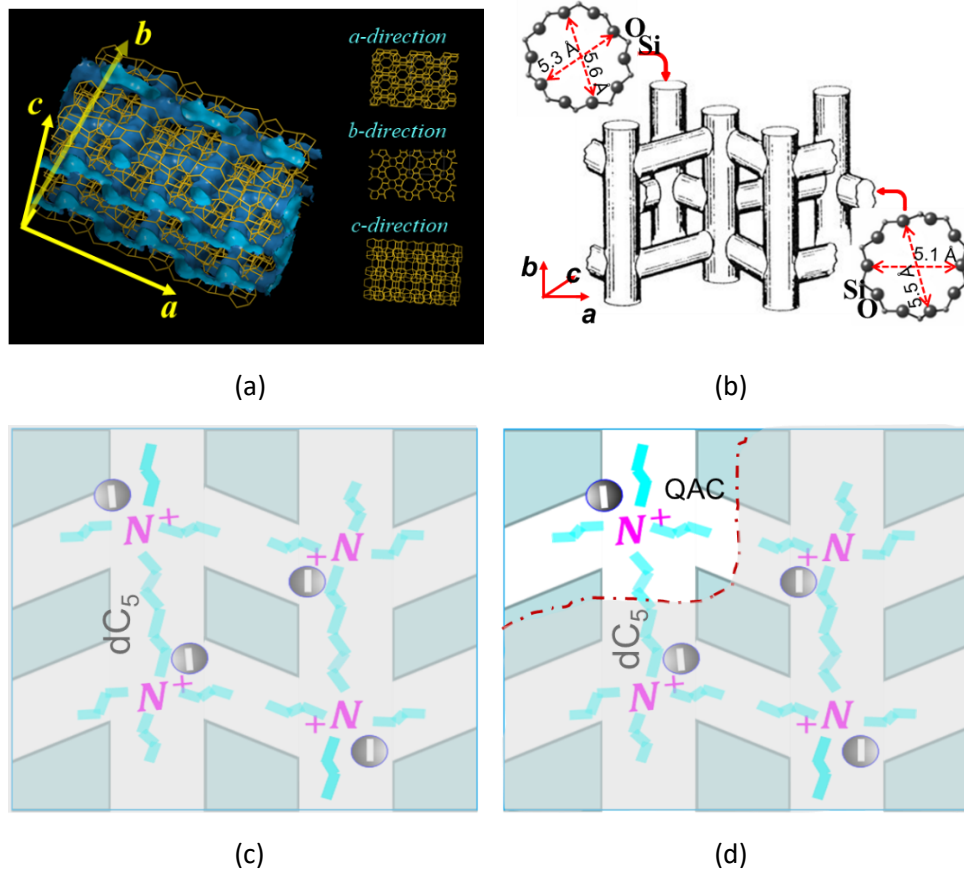

(a)

(b)

(c)

(d)

Fig. S2 Schematic showing the multi-step process for synthesizing the flat flakes of dC_5-templated silicalite nanosheets (SNs): (1) in-situ hydrothermal crystallization of a precursor with molar compositions of 10 SiO_2: 2.4 TPAOH: 0.87 NaOH: 114 H_2O to obtain the solution for seed synthesis; (2) precursor recovery after first reaction at 50 °C in an autoclave for 6 days; (3) the second in-situ crystallization of the filtered precursor at 140 °C for 2 days to generate spherical silicalite seeds of ~30 nm dia. [1]; (4) preparation of reaction mixture containing the 30-nm-dia. silicalite nano-seeds in a precursor sol with molar compositions of 80 TEOS: 3.75 dC_5: 20 KOH: 9500 H_2O; (5) seeded secondary growth at 140°C under autogenous pressure for 3.5 – 4.0 days to form rhombus-shaped SN crystals; (6) recovery of rhombus SNs by centrifugation after washing by KOH/KCl solution; (7) disintegration of rhombus-shaped flat crystals by sonication-assisted ball-milling and subsequent sedimentation fractionation to remove the chunky debris of the seed-evolved cores; and (8) extensive cleaning of the separated flat SNs by alternate washing with 0.1M KOH/KCl and 0.1M HCl/KCl solutions and filtration recovery and redispersion of SNs in ethanol at a SN content of ~ 0.2 wt.%. [2]
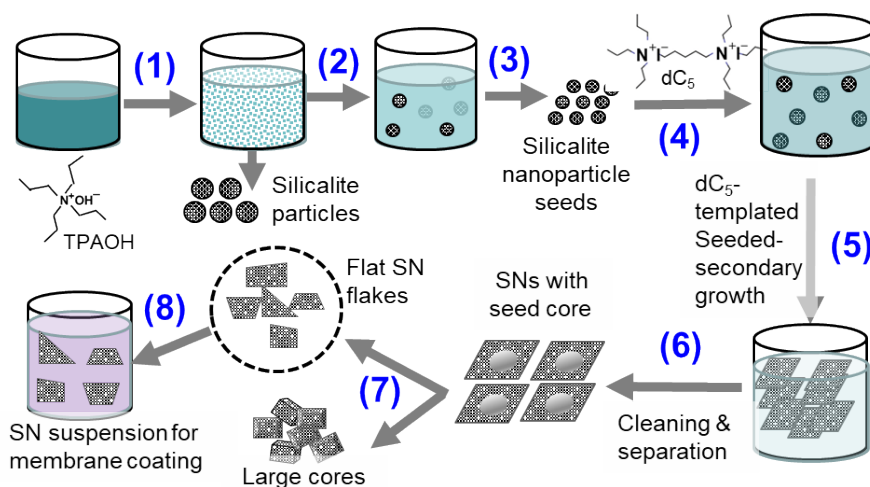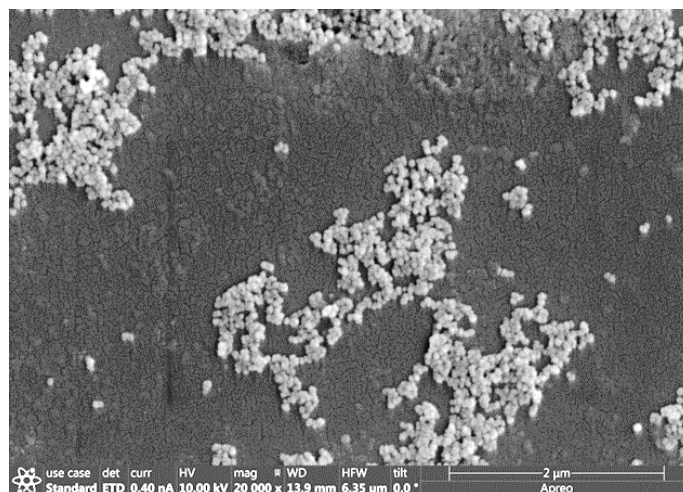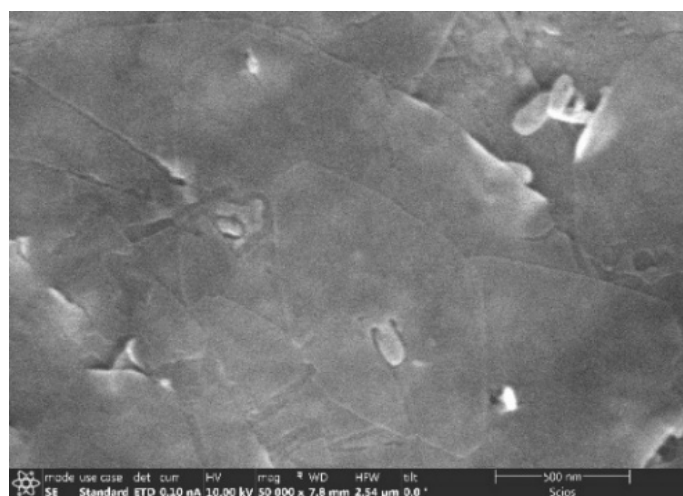
Fig. S3 (a) The silicalite nanoparticle seeds for hydrothermal secondary growth of the SNs using dC_5 template molecules and (b) the as-synthesized rhombus-shaped SNs containing seed-evolved thick cores.

(a)

(b)

Fig. S4 The photographs of (a) the vacuum filtration coating (VFC) apparatus for membrane fabrication and (b) a fresh SNLM-PVDF membrane obtained by the VFC process.
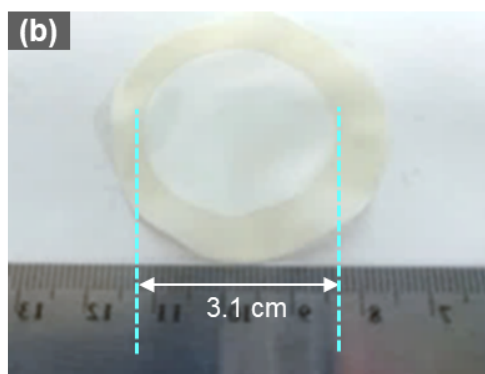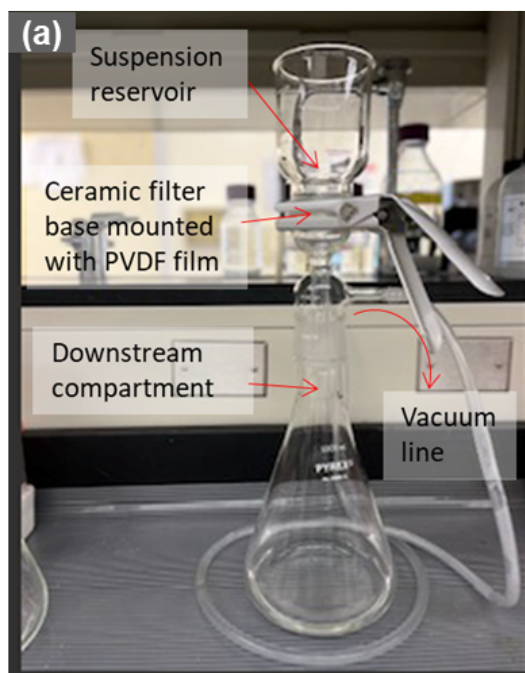
Fig. S5 (a) Schematic showing the AEM WE test system, (b) photo of cell assembly, and (c) photo of the disassembled WE cell displaying the cell components. The SNLM-PVDF was pre-treated by soaking in a 1M H_3PO_4 solution for 48 h followed by washing in DI water and then immersed in a 1M KOH solution at room temperature. The membrane was cleaned by DI water before making the membrane-electrode assembly (MEA). The AEM ASR is determined by comparing the resistances of the cell measured by EIS under identical conditions with AEM ($R_{cell\ with\ AEM}$) and without the AEM ($R_{cell\ without\ AEM}$), i.e., $ASR = (R_{cell\ with\ AEM} - R_{cell\ without\ AEM}) \cdot A_m$ where A_m is the AEM area being measured. The ASR of the SNLM layer is estimated by comparing the ASR of the SNLM-PVDF and that of the PVDF substrate alone. For determination of WE Coulombic efficacy, the H_2 gas production flowrate (r_{H2}) are measured by accumulative flowmeter over time t: $r_{H2} = pV_{H2}/(tRT)$ (mol/s) where p, V_{H2}, and T are pressure, volume, and temperature of the accumulated H_2 gas over a time t.
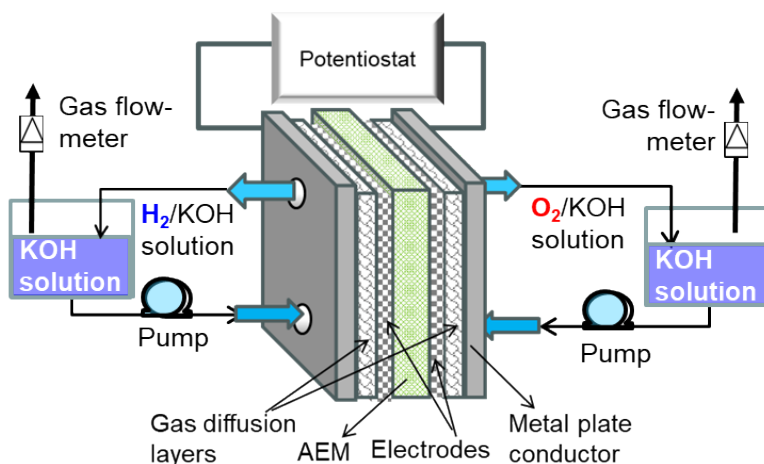
(a)
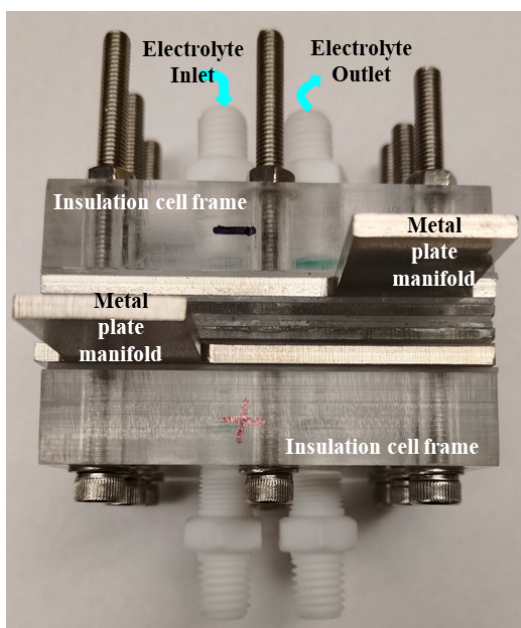
(b)
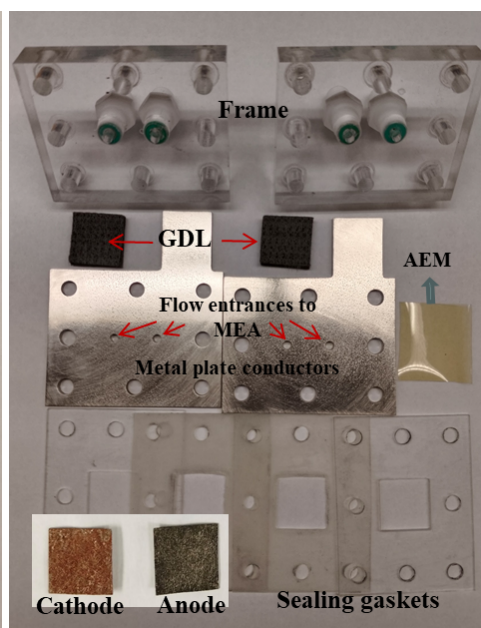
(c)

Fig. S6 SEM images of (a) the bare Ni felt, (b) the NiFe$_2$O$_4$-loaded Ni-felt anode before 120-h WE operation, (c) the anode after 120-h WE operation, (d) the Pt/C-loaded Ni-felt cathode before 120-h WE operation, and (e) the cathode after 120-WE operation. The catalyst ink for coating the cathode was a mixture of 190 μL of DI water and isopropyl alcohol (IPA) (1:1), 60 μL of Nafion solution (5 wt.% in IPA), and 5 mg of NiFe$_2$O$_4$ (or Pt/C) powders that was intensively dispersed by ultrasonication. The catalyst loading was done by carefully spreading 100 μL ink onto the nickel felt followed by drying in an oven at 60 °C for 12 h.

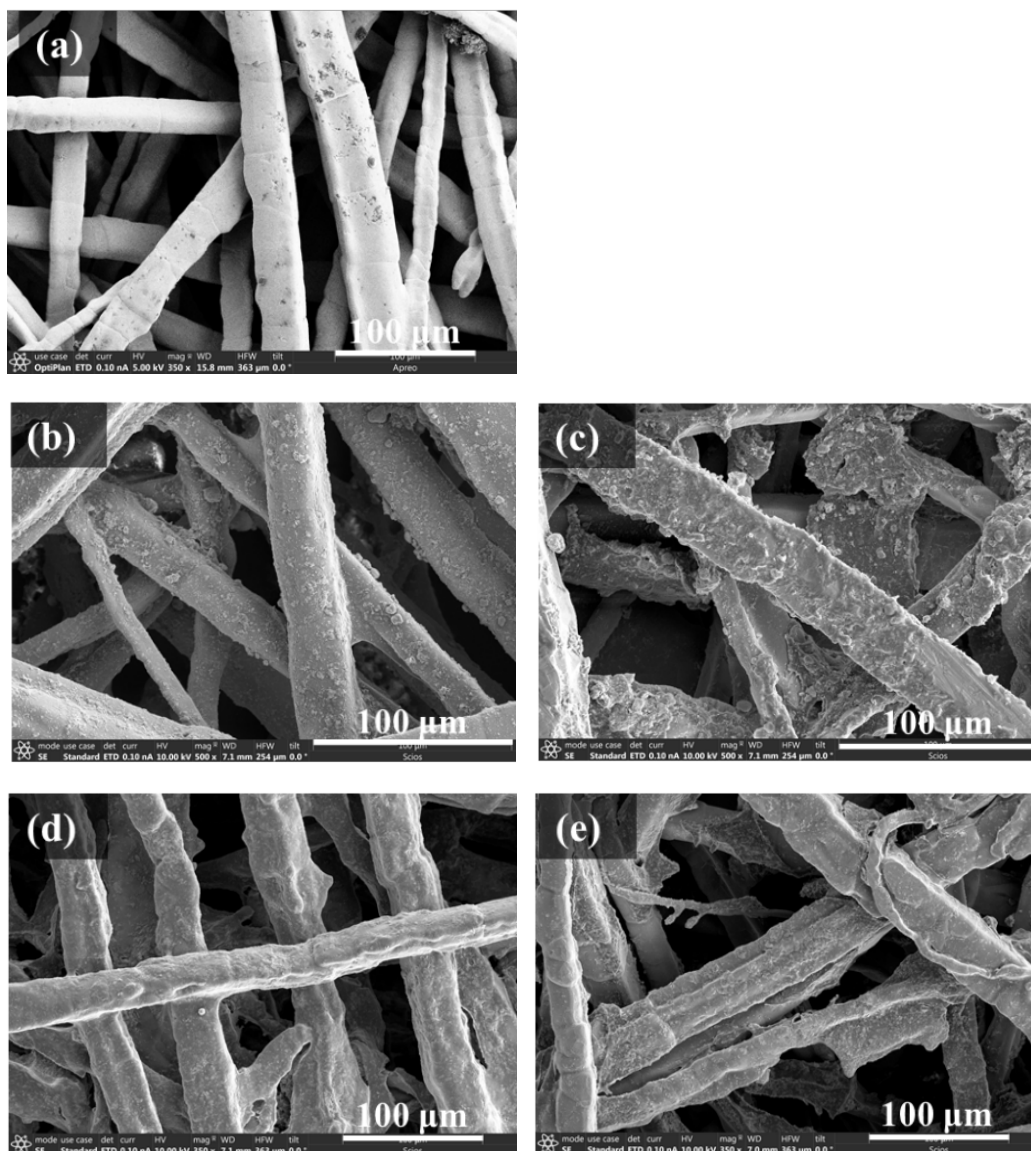**Fig. S7** (a) A low-magnification SEM image of the cross-section showing uniform SNLM thickness (~ 1.0 µm) on the porous PVDF film and (2) Strains-stress tests for PVDF, SNLM-PVDF, and FAA3-50 membranes performed in ambient air at room temperature (Instron 5948, ITW Test and Measurements) using samples prepared by hollow die punching (dimension of 40 mm × 10 mm).
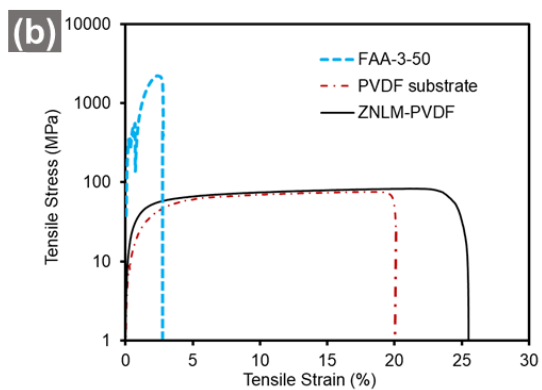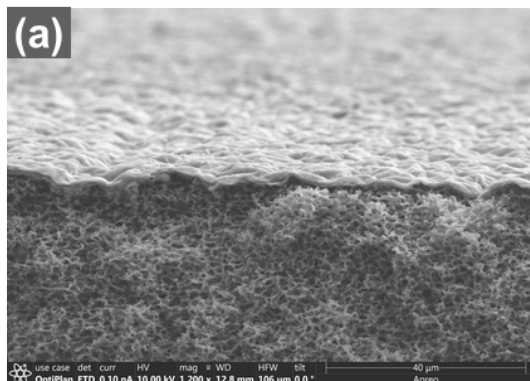
Fig. S8 XRD spectra of the standard silicalite powers, randomly parked SNs, layered SN film deposited on a glass wafer, porous PVDF film substrate, and the SNLM-PVDF. The exact match between the spectra of the randomly packed SNs and the silicalite powder standard confirms the MFI crystal structure purity of the SNs. The notable (020) peak and the absence of peaks of other planes in the XRD spectrum of the SNLM-PVDF indicates the achievement of a SNLM layer horizontally aligned in the a-c plane (i.e., b-direction oriented along the SN thickness). The broad hump around the (303) peak position can be attributed to the diffraction from wrinkled surface of the SNLM-PVDF that is not seen in the glass-supported multilayered SN film.
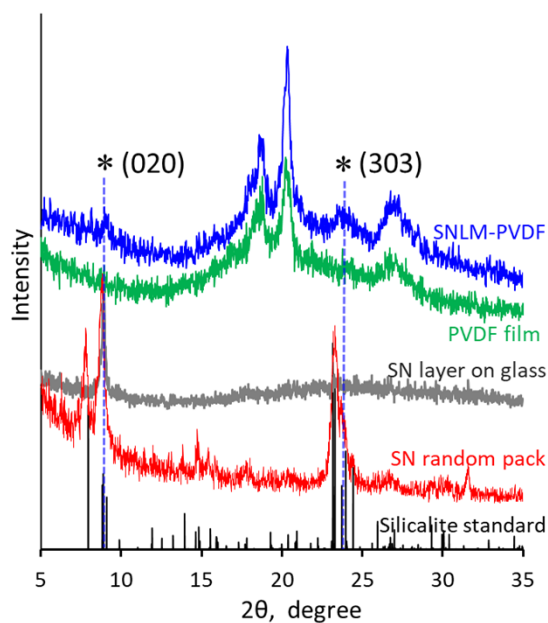
Fig. S9 Results of a repeated SNLM-PVDF test for WE with 5% KOH at 60°C and 400 mA/cm^2 over 360 h.

Chemicals, materials, and instruments:

Chemicals: All chemicals were used as-received without further purification or processing that include1,5 diaminopentane (98%, Alfa Aesar), iodopropane (99%, Sigma-Aldrich), 2-butanone (≥99.0%, Sigma Aldrich), potassium hydroxide (99.99%, Sigma-Aldrich), sodium hydroxide (99.99%, Sigma-Aldrich), potassium carbonate (anhydrous, ≥99%, Sigma-Aldrich), silicic acid (99.9%, 20 μm, Sigma Aldrich), ethyl acetate (anhydrous, 99.8%, Sigma-Aldrich), potassium chloride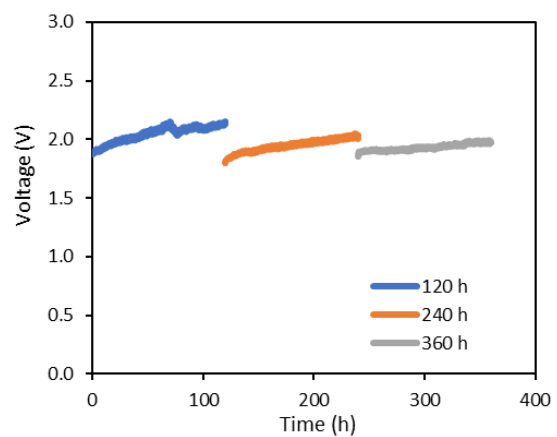 (anhydrous, ≥99%, Sigma-Aldrich), ethyl alcohol (200 proof, Sigma-Aldrich), tetrapropylammonium hydroxide (1M, aqueous, Sigma-Aldrich), tetraethyl orthosilicate (TEOS, >99.0%, Sigma-Aldrich), Dimethyl sulfoxide (DMSO, >99.7%, Sigma-Aldrich), and hydrochloric acid (37%, ACS reagent, Millipore Sigma). The dC_5 was homemade by following the literature procedure detailed in our previous work [1,2].

Materials: Materials used for membrane fabrication included the hydrophilic PVDF sheets for substrates (SF18140, pore size d_p = 0.45 μm, thickness δ = 0.125 μm, porosity ε = 0.8, TISCH Scientific, Ohio, USA), PVDF powders for binder (Kynar Flex® 2801-00, Arkema Inc., USA), $NiFe_2O_4$ nanoparticles (<50 nm particle size, ≥98% trace metal base, Millipore Sigma), Pt/C catalyst (Vulcan XC-72R, Fuel Cell Store), and nickel felt (L-STF, Bolin Metal Wire Mesh Co., China).

Instruments: The instruments employed for material characterization and test of the membrane properties included: transmission electron microscope (TEM, JEOL 2010F FE electron microscope); field emission electron scanning microscope (SEM, FEI Apreo SEM, ThermoFisher Scientific, USA); $\zeta-$potential analyzer (ZetaPlus®, Brookhaven Instrument, CT, USA); X-ray diffraction (XRD, PANalytical X'Pert Pro diffractometer with CuKα radiation λ=1.5406 Å); attenuated total reflectance Fourier transform infrared spectroscope (ATR-FTIR, Thermo Scientific Nicolet iS50 FT-IR spectrometer, Thermo Scientific, USA); strain-stress tester (Instron 5948, ITW T&M, USA).

Procedures for chemical and material syntheses and membrane fabrication

1. *Synthesis of bis-1,5(tripropyl ammonium) pentamethylene diiodide (dC$_5$)*

   a) Add 225 ml 2-butanone, 9.45 g 1,5-diaminopentane and 41.18 g anhydrous potassium carbonate to a three-neck round-bottom flask.
   b) Heat up the flask to 80°C under vigorous stirring in an oil bath on a hot plate; use argon purging at 50ml/min to obtain an inert atmosphere in the flask and keep flushing during the reaction under water-cooled refluxing; keep the flask wrapped up with aluminum foil to avoid iodide oxidation.
   c) Add 54 ml of 1-iodopropane dropwise into the reaction mixture in the flask.
   d) Terminate the reaction after 10 h of reaction under the above conditions.
   e) After cooling down, use filtration to remove the potassium salts and retrieve the liquid product.
   f) Evaporate liquid product at 80 °C in the oil bath under stirring to remove 2-butanone.
   g) Dissolve the product in 125 ml of 2-butanone and stir for 1 h; then add 125 mL ethyl acetate and stir for overnight; filter the resultant mixture to recover solid powder product.
   h) Dissolve the recovered solid in the minimum amount of 200 proof ethanol and stir until it is fully dissolved then remaining KI is filtered.
   i) Recover the filtrate products by evaporation on hot plate.
   j) Repeat the purification process of step (g) – step (i) for 4 times to obtained final product of dC$_5$.

2. *Preparation of silicalite nanoparticle seeds for SN synthesis*
   a) Prepare a precursor sol with molar compositions of 10SiO$_2$:2.4TPAOH:0.87NaOH:114H$_2$O by
      I. Add 0.16 g water, 0.127 g of sodium hydroxide and 8.93 g of 1.0 M TPAOH solution into a Teflon flask,
      II. Stir the above mixture for 5 min to obtain a homogeneous solution and then 2.5 g of silicic acid is added into the solution,
      III. The solution was kept at room temperature under stirring for overnight.
   b) Perform in-situ hydrothermal crystallization to form nanocrystalline silicalite particles by
      I. Put the capped precursor-containing flask into an oven preheated to 50 °C,
      II. Conduct hydrothermal crystallization under static condition for 6 days,
   c) Terminate the hydrothermal crystallization and filter the resultant suspension with a GHP syringe filter (pore size 0.45 µm) to remove the particulate products and recover the liquid phase product
   d) Put the recovered liquid filtrate in Teflon lined autoclave and perform a second hydrothermal crystallization at 100 °C for 3 days.
   e) Recover silicalite nanoparticle product by centrifugation and DI water cleaning. The centrifugation and DI water redispersion is repeated until the suspension pH is close to 7. The solid was re-dispersed in DI water by sonication.
   f) Determine the solid content of the seed crystal suspension by weighing the solid dried from 10-g suspension.

3. *Silicalite nanosheet (SN) synthesis*
   a) The precursor solution for secondary growth of SN has molar compositions of 80 TEOS : 3.75 dC$_5$: 20 KOH : 9500 H$_2$O by mixing 3.90 g TEOS, 0.536 g dC5, 0.262 g KOH, and 40 g H$_2$O in a flask under stirring.
   b) Purge the solution with Ar (50 ml/min) at room temperature for 16 h to reduce ethanol content.
   c) Filter the precursor sol with the GHP syringe filter (pore size 0.45 µm) to recover the liquid precursor.

d) Place the precursor sol in a flask and add the seed crystal suspension into this precursor to achieve a silica-based molar ratio between the seed suspension and the precursor sol of 1:200. The seed suspension added contains 40 g H_2O and 5.6 mg of silicalite nanoparticle seeds.

e) Transfer the silicalite nanoparticle seeded precursor into a Teflon lined autoclave

f) Conduct hydrothermal secondary growth at 140 °C for 3.5 to 4 days under autogenous pressure.

g) Centrifuge to recover the solid product and wash the nanosheet product to remove the residual amorphous silica. The solution for washing the SN product contains 0.1 M KOH and 1 M KCl. The centrifugation and washing process is repeated for 3 times

h) Rinse the solid products with DI water through centrifugation and redispersion until pH close to 7. The resultant solid is dispersed in DI water or EtOH for processing to recover flat SNs.

4. *Fabrication of SNLM-PVDF*

a) The suspension for membrane VFC coating contained 0.02wt.% SN and 0.06wt.% of dissolved PVDF in a mixed solvent, which had an EtOH:DMSO weight ratio of 2:1. The suspension was prepared by mixing the 0.2 wt.% SN suspension in EtOH (Fig. S2) with a calculated amount of PVDF binder solution (in the EtOH+DMSO mixed solvent). The 0.02 wt.% SN content was identified to ensure sufficient SNs for forming a pinhole-free compact SNLM layer, and the specific solvent composition (67wt.% EtOH+33wt.% DMSO) was optimized to fully dissolve the PVDF binder while avoiding dissolving or damaging the PVDF substrate during the vacuum filtration coating (VFC) process. [2]

b) The porous PVDF film support was soaked with EtOH when mounted in the VFC coating apparatus to prevent misalignment of SN that could be caused by strong capillary suction from a dry porous PVDF substrate.

c) The SN suspension was intensively sonicated for 20 min before being charged into the suspension reservoir for VFC membrane formation.

d) The SNLM was coated by total filtration of 3-mL of the SN suspension over a circular area of 7.55 cm^2.

e) The freshly SNLM-PVDF was immediately dried in a vacuum oven at 80°C and ~1.5 kPa for 2 h and subsequently cured at 120 °C and ~ 24 kPa for 3 h.

Table S1: AEM-WE performance of recently established AEMs

Anode	Cathode	Performance	Membrane	Temp (°C)	C_{KOH}	Ref.
IrO_2 (2)	Pt/C (2)	1000 mA cm^{-2} at 2.15 V	Fumasep FAA-3-50	60	1 M	3
$NiMn_2O_4$	Pt/C (0.5)	530 mA cm^{-2} at 2.0 V	Fumasep FAA-3-50	80	1 M	4
IrO_2	Pt/C	1000 mA cm^{-2} at 2.65 V	Fumatech FAA3-PK-75	60	1 M	5
NiFe	Ni	300 mA cm^{-2} at 2.0 V	Sustainion X37-50	40	1 M	6
CuCoO	NiCoONiCo/C	504 mA cm^{-2} at 1.8 V	Sustainion X37-50	60	1 M	7
IrO_2 (4.0)	Pt/C (4.0)	500 mA cm^{-2} at 1.72 V	A901 (Tokuyama)	70	1 M	8
nickel felt	nickel felt	500 mA cm^{-2} at 2.3 V	Aemion™	60	1 M	9
Ni foam (Bekaert)	Pt/C (0.5)	0.62 A cm^{-2} at 2 V	PiperION™ (Versogen)	60	1 M	10
IrO_2	Pt/C	368 mA/cm^2 at 2.1 V	PBI with norborene	60	1 M	11
Pt/C	Ir black	700 mA cm^{-2} at 2 V	PBI1-PVBC1-NMPD/ OH	60	1 M	12
Pt/C	Ir black	680 mA cm-2 at 2 V	SEBS-P206	60	0.1 M	13
IrO_2	Pt/C	547 mA/cm^{-2} at 2.0 V	PISPVA46	60	0.5 M	14
Pt/Ru	Pt	400 mA cm^{-2} at 2.5 V	PAImEE	60	6 M	15
IrO_2	Pt/C	620 mA cm^{-2} at 2.0 V	FAA-3-50	60	1 M	16
$NiMn_2O_4$/CNF	Pt/C	130 mA cm^{-2} at 1.8 V	FAA3-50	50	6 M	17
$NiMn_2O_4$/CNF	Pt/C	100 mA cm^{-2} at 1.8 V	FAA3-50	60	6 M	17
$NiMn_2O_4$/C	Pt/C	380 mA cm^{-2} at 2.0 V	FAA-3-50	50	1 M	18
Ni foam	Ni foam	150 mA cm^{-2} at 2.0 V	Aquivion-based	80	3 M	19
Ni foam	Ni foam	130 mA cm^{-2} at 2.0 V	AEMION	80	3 M	19
Ni foam	Ni foam	0.03 A cm^{-2} at 2.0 V	FAA-3-50	60	10wt%	20
IrO_2	Pt/C	460 mA cm^{-2} at 1.8 V	FAA3-PK-75	50	0.5 M	21
IrO_2	Pt/C	630 mA cm^{-2} at 1.8 V	FAA3-PK-75	70	0.5 M	21
Ni foam	Ni foam	335 mA cm^{-2} at 2.0 V	C-ABPBI	70	16.5wt%	22
$NiFe_2O_4$ (2)	Pt/C (0.5)	523 mA cm^{-2} at 2.00 V	SNLM-PVDF	60	5wt%	This work
$NiFe_2O_4$ (2)	Pt/C (0.5)	3000 mA cm^{-2} at 2.35 V	SNLM-PVDF	60	25wt%	This work

Refrences:

[1]   M.Y. Jeon, D. Kim, P. Kumar, P.S. Lee, N. Rangnekar, P. Bai, M. Shete, B. Elyassi, H.S. Lee, K. Narasimharao, S.N. Basahel, S. Al-Thabaiti, W. Xu, H.J. Cho, E.O. Fetisov, R. Thyagarajan, R.F. Dejaco, W. Fan, K.A. Mkhoyan, J.I. Siepmann, M. Tsapatsis, Ultra-selective high-flux membranes from directly synthesized zeolite nanosheets, Nature 543 (2017) 690-694.

[2]   Z. Cao, L. Iskhakova, X. Sun, Z. Tang, J. Dong, ZSM-5 Zeolite Nanosheet-Based Membranes on PorousPolyvinylidene Fluoride for High-Flux Desalination, ACS Appl. Nano Mater. 4 (2021) 2895–2902.

[3]   L. Wan, Z. Xu, B. Wang, Green preparation of highly alkali-resistant PTFE composite membranes for advanced alkaline water electrolysis, Chem. Eng. J. 426 (2021) 131340.

[4].   A. Carbone, S.C. Zignani, I. Gatto, S. Trocino, A.S. Aricò, Assessment of the FAA3-50 polymer electrolyte in combination with a NiMn2O4 anode catalyst for anion exchange membrane water electrolysis, Int. J. Hydrogen Energy. 45 (2020) 9285-9292.

[5].   I. Vincent, A. Kruger, D. Bessarabov, Development of efficient membrane electrode assembly for low cost hydrogen production by anion exchange membrane electrolysis, Int. J. Hydrogen Energy. 42 (2017) 10752-10761.

[6]   E. López-Fernández, C. Gómez-Sacedón, J. Gil-Rostra, J.P. Espinós, J.J. Brey, A.R. González-Elipe, A. de Lucas-Consuegra, F. Yubero, Optimization of anion exchange membrane water electrolyzers using ionomer-free electrodes, Renew. Energy. 197 (2022) 1183-1191.

[7]   Y.S. Park, J. Jeong, Y. Noh, M.J. Jang, J. Lee, K.H. Lee, D.C. Lim, M.H. Seo, W.B. Kim, J. Yang, S.M. Choi, Commercial anion exchange membrane water electrolyzer stack through non-precious metal electrocatalysts, Appl. Catal. B Environ. 292 (2021) 1-9.

[8]   Y. Pan, J. Zhang, Z. Zhao, L. Shi, B. Wu, L. Zeng, Iron-doped metal-organic framework with enhanced oxygen evolution reaction activity for overall water splitting, Int. J. Hydrogen Energy. 46 (2021) 34565-34573.

[9]   A. Khataee, A. Shirole, P. Jannasch, A. Krüger, A. Cornell, Anion exchange membrane water electrolysis using Aemion™ membranes and nickel electrodes, J. Mater. Chem. A. 10 (2022) 16061-16070.

[10]   L. Xia, W. Jiang, H. Hartmann, J. Mayer, W. Lehnert, M. Shviro, Multistep Sulfur Leaching for the Development of a Highly Efficient and Stable NiSx/Ni(OH)$_2$/NiOOH Electrocatalyst for Anion Exchange Membrane Water Electrolysis, ACS Appl. Mater. Interfaces. 14 (2022) 19397-19408.

[11]   M. Guo, T. Ban, Y. Wang, X. Wang, X. Zhu, "Thiol-ene" crosslinked polybenzimidazoles anion exchange membrane with enhanced performance and durability, J. Colloid Interface Sci. 638 (2023) 349-362.

[12]   W. Lu, Z. Yang, H. Huang, F. Wei, W. Li, Y. Yu, Y. Gao, Y. Zhou, G. Zhang, Piperidinium-Functionalized Poly(Vinylbenzyl Chloride) Cross-linked by Polybenzimidazole as an Anion Exchange Membrane with a Continuous Ionic Transport Pathway, Ind. Eng. Chem. Res. 59 (2020) 21077-21087.

[13]   Z. Xu, V. Wilke, J.J. Chmielarz, M. Tobias, V. Atanasov, A.S. Gago, K.A. Friedrich, Novel piperidinium-functionalized crosslinked anion exchange membrane with flexible spacers for water electrolysis, J. Memb. Sci. 670 (2023) 121302.

[14]   H.J. Park, S.Y. Lee, T.K. Lee, H.J. Kim, Y.M. Lee, N$_3$-butyl imidazolium-based anion exchange membranes blended with Poly(vinyl alcohol) for alkaline water electrolysis, J. Memb. Sci. 611

(2020) 118355.

[15]   J. Fan, S. Willdorf-Cohen, E.M. Schibli, Z. Paula, W. Li, T.J.G. Skalski, A.T. Sergeenko, A. Hohenadel, B.J. Frisken, E. Magliocca, W.E. Mustain, C.E. Diesendruck, D.R. Dekel, S. Holdcroft, Poly(bis-arylimidazoliums) possessing high hydroxide ion exchange capacity and high alkaline stability, Nat. Commun. 10 (2019) 2306.

[16]   J.E. Park, M.J. Kim, M.S. Lim, S.Y. Kang, J.K. Kim, S.H. Oh, M. Her, Y.H. Cho, Y.E. Sung, Graphitic carbon nitride-carbon nanofiber as oxygen catalyst in anion-exchange membrane water electrolyzer and rechargeable metal–air cells, Appl. Catal. B Environ. 237 (2018) 140-148.

[17]   C. Busacca, S.C. Zignani, A. Di Blasi, O. Di Blasi, M. Lo Faro, V. Antonucci, A.S. Aricò, Electrospun $NiMn_2O_4$ and $NiCo_2O_4$ spinel oxides supported on carbon nanofibers as electrocatalysts for the oxygen evolution reaction in an anion exchange membrane-based electrolysis cell, Int. J. Hydrogen Energy. 44 (2019) 20987-20996.

[18]   A. Carbone, S.C. Zignani, I. Gatto, S. Trocino, A.S. Aricò, Assessment of the FAA3-50 polymer electrolyte in combination with a $NiMn_2O_4$ anode catalyst for anion exchange membrane water electrolysis, Int. J. Hydrogen Energy. 45 (2020) 9285-9292.

[19]   P. Stilli, S. Bonizzoni, F. Lohmann-Richters, L. Beverina, A. Papagni, P. Mustarelli, Aquivion®-based anionic membranes for water electrolysis, Electrochim. Acta. 405 (2022) 139834.

[20]   N. Lee, D.T. Duong, D. Kim, Cyclic ammonium grafted poly (arylene ether ketone) hydroxide ion exchange membranes for alkaline water electrolysis with high chemical stability and cell efficiency, Electrochim. Acta. 271 (2018) 150-157.

[21]   A. Lim, H. juhn Kim, D. Henkensmeier, S. Jong Yoo, J. Young Kim, S. Young Lee, Y.E. Sung, J.H. Jang, H.S. Park, A study on electrode fabrication and operation variables affecting the performance of anion exchange membrane water electrolysis, J. Ind. Eng. Chem. 76 (2019) 410-418.

[22]   L.A. Diaz, J. Hnát, N. Heredia, M.M. Bruno, F.A. Viva, M. Paidar, H.R. Corti, K. Bouzek, G.C. Abuin, Alkali doped poly (2,5-benzimidazole) membrane for alkaline water electrolysis: Characterization and performance, J. Power Sources. 312 (2016) 128-136.